Séminaire Poincaré XII (2009) 1 – 31 Séminaire Poincaré

Constructing Tools for the Description of Cell Dynamics

Jean-François Joanny
Institut Curie, CNRS UMR 168,
26, rue d'Ulm
75248 Paris Cedex 05 - France

Jacques Prost
Physicochimie Curie (CNRS-UMR168),
Institut Curie, Section de Recherche,
26, rue d'Ulm
75248 Paris Cedex 05 - France
&
E.S.P.C.I,
10 rue Vauquelin,
75231 Paris Cedex 05 - France

Abstract. We give a survey of the work which we and others have done over the last years on "active gels". In particular, we show how one can construct a set of equations describing gels in which the cross-links can be moved around by active elements constantly consuming energy. This situation corresponds to the cell cytoskeleton, which is thought to control most of cell dynamics. We illustrate the potential usefulness of the equations first by giving material science type of applications, second by discussing cell behavior such as motility, oscillations, wound healing and cytokinesis.

1 Introduction

Our knowledge in Biology has improved significantly over the last fifty years, with impressive successes in molecular biology, genetics, developmental and cell biology. The wealth of information is such that it is hard to make use of all of them. Although it is clear that details matter in biological systems, it is also clear that one currently needs to develop a global picture taking into account the main features and recognizing what is universal. Cell biology provides a good example of this need: with exactly the same genome cells can differentiate in about three hundred different types in complex animals such as vertebrates [1]. Physicists would say that they can go to three hundred stable attractors depending on external conditions. Considering that cell phase space is controlled among other things by the expression of a few 10^4 genes, three hundred is a very small number. A possible explanation for this small number of cell types is that they are not only controlled by gene expression, but that they are also constrained by generic physical laws. We are far from being able to discuss this problem in its generality, but in the following

we address a simpler problem which illustrates how physics could provide generic tools for raising these questions. Namely we investigate what can be learned from using symmetry arguments and conservation laws in describing cell morphology and dynamics. In view of the acknowledged specificity of biology such an endeavor may seem futile. We hope to convince the reader that it is on the contrary helpful. Indeed we will discuss in the last three sections of this review:

-one simple aspect of cell motility, namely the shape and speed of a lamellipodium, thin protrusion leading the cell motion on a substrate,

-cell oscillations which are observed when cells are suspended in a physiological serum,

-wound healing of xenopus eggs and the onset of cytokinesis.

For all these examples we use the the same theoretical framework.

In order to do so, one needs to construct the tools. It is nowadays textbook knowledge that the shape of cells is maintained by a network of cross-linked biofilaments: the cytoskeleton [2]. At this stage, all we need to know is that the network constitutes a physical gel which would be rather conventional in the absence of molecular motors. At short time scales, it behaves like a conventional solid, at long time scales like a liquid. There are in fact some added complexities which will be discussed in the conclusion. The essential novelty comes from molecular motors. They consume continuously ATP (Adenosine Triphosphate) and are able to exert stresses on the cross-links of the gel. The question is then how to describe such a gel, which we call "active". Using conservation laws and symmetry arguments only we derive the relevant equations in section II. Since they result from general considerations these equations can describe many different situations and are very similar to those derived in different contexts such as motions of bacterial colonies, fish shoals and bird flocks [3, 4, 5]. Active gels could also be made artificially, leading to original material properties [6]. In the third section, we discuss some of these expected original properties, such as the spontaneous transition to a moving state of a thin slab and the rotation of disclinations.

In the fourth, fifth and sixth sections we discuss the already mentioned biologically relevant questions, showing how quantitative information can be obtained and how connection with molecular details can be made. In the last section, we discuss the limitations and merits of the present construction.

2 Hydrodynamic theory of active gels

A common attitude for dealing with the cytoskeletal system in the presence of motors is to simulate ensembles of semi-flexible filaments on which motor bundles can exert force dipoles [7, 8]. Although, this is perfectly licit and useful, it does not help much to extract generic behaviors. Another possibility is to start from a molecular picture and get from a statistical description the long wavelength, long time scale equations [9, 10, 11, 12]. This task is difficult: the low density limit has been worked out, without keeping track of the embedding solvent. In a pragmatic at-

titude, one can directly write equations including all terms allowed by symmetry as has been done for bacterial colonies and bird flocks [3, 4] but it is not guaranteed that one expands equations around an existing state [13].

We have chosen to use generalized hydrodynamics. Hydrodynamic theories have been very successful in the description of systems such as superfluids, liquid crystals, polymers and of course simple fluids. They are valid close to equilibrium. The advantage is that the equations are expanded around a well defined state. The drawback is that biological systems are not close to equilibrium: one might miss biologically relevant terms. We will discuss such a candidate in the following. In order to build a hydrodynamic theory, one has to identify conserved quantities, and continuous broken symmetries. From there on, the procedure is well defined and systematic. We will not go here through all the steps, referring the reader to references [14, 15, 16].

Conserved quantities are fairly easy to identify: the solvent, the cytoskeleton (actin in practice), the motors and most importantly momentum. Two added complexities though. First, actin units are either in the solvent as monomers or belong to polymerized filaments. There is, a priori, a chemical exchange between the two states, described by rates of polymerization and depolymerization. The corresponding biochemistry is well documented and original. We postpone its description to the discussion of biological examples. Second the motors can be either bound to the filaments or unbound. This means that in principle the minimal description is that of a five-component system! One has to further identify continuous broken symmetries: actin filaments are polar, and most of the time even tough their directions are widely statistically distributed they define a common polar direction. This means that on long time scales the system behaves like a polar active nematic as described first by [3]. One has thus to keep a polar order parameter as well. Deep into the ordered phase it can be chosen as a unit vector $\mathbf{p}$.

In the following , we discuss a simplified version of the equations, in which we keep only the gel velocity field $\mathbf{v}$ and the polarization field $\mathbf{p}$. The validity range and limits of this approximation are currently being investigated.

Constitutive equations are obtained by first identifying the fluxes and the corresponding conjugate generalized forces. Constitutive relations are obtained by a general linear expansion of fluxes in terms of forces, writing all terms which are consistent with the symmetries of the system. For the conventional terms we follow the so called "Harvard choice", taking as flux the symmetric part of the stress tensor $\sigma_{\alpha\beta}$ and the "objective" polarization rate of change

$$P_\alpha = \frac{\partial p_\alpha}{\partial t} + v_\gamma \partial_\gamma p_\alpha + \frac{1}{2}(\partial_\alpha v_\beta - \partial_\beta v_\alpha) p_\beta, \tag{1}$$

and for forces, the symmetric strain rate

$$u_{\alpha\beta} = \frac{1}{2}(\partial_\alpha v_\beta + \partial_\beta v_\alpha), \tag{2}$$

and the orientational filed defined as the functional derivative of the free energy F with respect to the polarization $\mathbf{p}$.

$$h_\alpha = -\frac{\delta F}{\delta p_\alpha} \ . \tag{3}$$

The relevant part of the energy is the polarization free energy given by the standard expression for a polar liquid crystal [18] :

$$F = \int dxdy \left[\frac{K_1}{2}(\nabla \cdot \mathbf{p})^2 + \frac{K_2}{2}(\mathbf{p}.(\nabla \times \mathbf{p}))^2 + \frac{K_3}{2}(\mathbf{p} \times (\nabla \times \mathbf{p}))^{\mathbf{2}} - \frac{\mathbf{1}}{\mathbf{2}}\mathbf{h}_{\|}\mathbf{p}^{\mathbf{2}} \right] \tag{4}$$

where $K_1 = K$, K_2 and K_3 are the splay, twist and bend elastic moduli. We have introduced here a Lagrange multiplier $h_{||}$ in order to satisfy the constraint $\mathbf{p}^2 = 1$ and we have omitted surface terms such as the linear splay term which is specific to polar systems.

Of particular significance for our theory is the existence of active processes mediated by molecular motors. In general, a chemical fuel, such as Adenosinetriphosphate (ATP), provides the energy source. Motor molecules consume ATP by catalyzing the hydrolysis to Adenosinediphosphate (ADP) and inorganic phosphate and transduce the free energy of this reaction to generate forces and motion along filaments. The energy of ATP is also used in order to polymerize and depolymerize filaments. The presence of the fuel represents a chemical "force" acting on the system. We characterize this generalized force by the chemical potential difference $\Delta\mu$ of ATP and its hydrolysis products, ADP and inorganic phosphate. The corresponding flux is the ATP consumption rate r. We thus have the following set of fluxes and forces:

$$\begin{array}{rcl} \text{flux} & \leftrightarrow & \text{force} \\ \sigma_{\alpha\beta} & \leftrightarrow & u_{\alpha\beta} \\ P_\alpha & \leftrightarrow & h_\alpha \\ r & \leftrightarrow & \Delta\mu \ . \end{array} \tag{5}$$

After some manipulations we obtain the following constitutive equations [16]:

$$2\eta u_{\alpha\beta} = \left(1 + \tau\frac{D}{Dt}\right)\left\{\sigma_{\alpha\beta} + \zeta\Delta\mu(p_\alpha p_\beta - \frac{\delta_{\alpha\beta}}{3}) + \frac{\nu_1}{2}(p_\alpha h_\beta + p_\beta h_\alpha)\right\} \tag{6}$$

$$\frac{dp_\alpha}{dt} = -(v_\gamma\partial_\gamma)p_\alpha - \omega_{\alpha\beta}p_\beta - \nu_1 u_{\alpha\beta}p_\beta + \frac{1}{\gamma_1}h_\alpha + \lambda_1 p_\alpha\Delta\mu \tag{7}$$

$$r = \zeta p_\alpha p_\beta u_{\alpha\beta} + \Lambda\Delta\mu + \lambda_1 p_\alpha h_\alpha \quad . \tag{8}$$

Here we have included geometric non-linearities but we have restricted other terms to linear order in the logic of the expansion. Also, we have neglected chiral terms which in principle exist in cytoskeletal systems, and assumed an incompressible gel. Eq. (6) generalizes the expression of the stress tensor of a visco-elastic Maxwell gel to active systems with polarity. Indeed, if we first look at passive terms, i.e. those which survive

when $\Delta\mu = 0$, it is straightforward to check that the equation describes an elastic medium at short time scales, and an anisotropic fluid at long time scales, i.e. a nematic liquid. For the sake of simplicity we have introduced only one viscosity coefficient η and $\sigma_{\alpha\beta}$ is the traceless symmetric stress.The elastic modulus of the short time gel is $E = \frac{\eta}{\tau}$.

The term proportional to $\Delta\mu$ is the only novel term compared to passive systems. If all flows are suppressed, for instance by suitable boundary conditions (which is possible), the active terms generate a nonzero stress tensor. A contractile stress corresponds to $\zeta\Delta\mu < 0$, and a dilative stress to $\zeta\Delta\mu > 0$. In view of the fact that experiments show that the stress is contractile in the case of the actin-myosin system, [19, 20] we call $\zeta\Delta\mu$ the contractility of the system; it has the dimensions of an elastic modulus. If by another choice of suitable boundary conditions, the stress is maintained to zero, the active term generates spontaneous motion. We illustrate both these situations in the following. Thus, ATP hydrolysis can generate forces and material flow in the gel via the action of active elements such as motors. These effects are characterized by one coefficient ζ. Similarly, Eq. (7) describes the dynamics of a nematic liquid, with just one added term weighted by the coefficient λ_1. This term plays a role only if the degree of order is not fixed, since it is a longitudinal term. If the polarization field can be taken as a unit vector then this term does not change the physics. An other term implying gradients of the polarization is allowed by symmetry in Eq. (7), namely $p_\beta\partial_\beta p_\alpha$. Since this term does not appear in a passive system, the coefficient characterizing it must be proportional to $\Delta\mu$. It is thus a second order term, which should not be retained in the logic of a linear expansion. It appears however naturally in gradient expansions far from equilibrium [9, 21]. It is easy to realize that it favors sharp polarization gradients. In cases where this term is important, interesting structures are expected [22].

Furthermore, material flow couples to the polarization dynamics via the coefficients ν_1 . The rate of ATP consumption r is primarily driven by $\Delta\mu$ and characterized by Λ. However, it is also coupled to the fluid flow and to the field $\mathbf{h}$ acting on $\mathbf{p}$.

These equations are complemented by the force balance condition:

$$\partial_\beta \sigma^{tot}_{\alpha\beta} = \partial_\beta \Pi \tag{9}$$

where Π is the pressure and $\sigma^{tot}_{\alpha\beta} = \sigma_{\alpha\beta} + \frac{1}{2}(p_\alpha h_\beta - p_\beta h_\alpha)$. This last relation is familiar to liquid crystal physics and results from rotational invariance.

3 Material Science Aspects

If one specializes Eq. (7), to steady state in the passive case of a nematic liquid submitted to the action of a simple shear $\frac{\partial v_x}{\partial y}$ one finds that, in the absence of any other orienting field or boundary effect, the nematic director picks a well defined and stable direction making an angle θ with the y axis such that $cos(2\theta) = \frac{1}{\nu_1}$ whenever $-1 < \frac{1}{\nu_1} < 1$ (1). This means that the shear flow exerts a torque on the nematic director until it reaches that direction. This flow alignment, has been well characterized

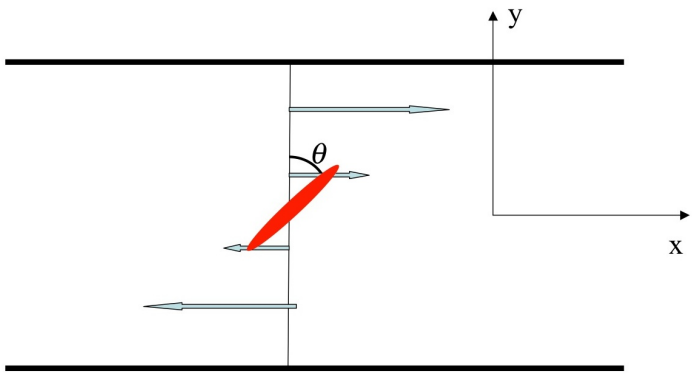

Figure 1: Alignment of a nematic director in a simple shear, as described in the text.

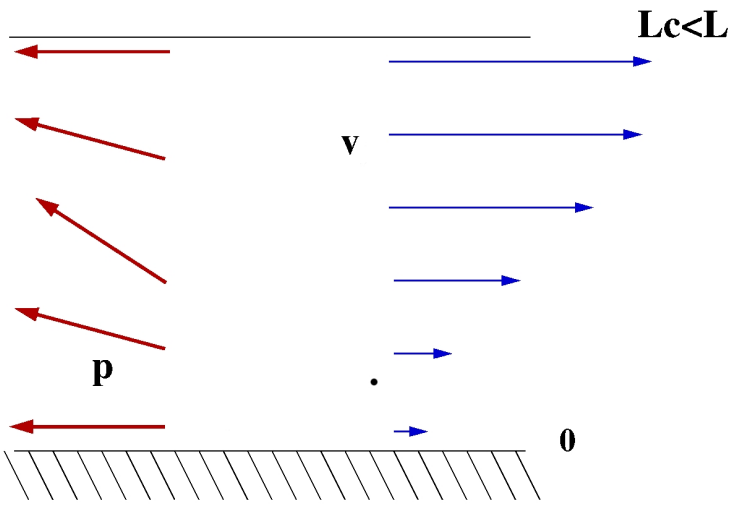

Figure 2: Spontaneous distorsion (left) and flow field(right) of an initially homogeneous slab, with a free upper surface and parallel boundary conditions for the polarization.

in nematics (it plays often an unwanted role in display devices). This term is still present in the active polar case and the same shear will have the same tendency to orient the polarization direction.

Conversely, Eq.(6) shows that in the absence of stress, a polarization tilt tends to result in a shear. One can thus understand, that with appropriate signs of the coupling terms, a possibility for a dynamical instability exists.

One can for instance look at a slab geometry with a free surface, and in which the polarization field is oriented parallel to the surfaces in a direction which we call y. We call x the normal to the slab surface. The free surface guarantees that for any perturbation with zero wavevector parallel to the slab the σ_{yx} stress vanishes. In the absence of activity

$\zeta\Delta\mu = 0$ we know from thermodynamics that the homogeneous state with the polarization parallel to the faces of the slab is the lowest energy state. It is thus stable. Now, let us slowly increase activity. For small activity, the system is still stable. However, for a well defined critical activity threshold, simultaneously the polarization field becomes inhomogeneous and a shearing motion sets in. This situation is reminiscent of the Frederiks transition: when a nematic liquid initially homogeneously aligned in direction$y$, is submitted to the action of a magnetic field oriented in direction x, it starts to distort under the action of the field only after a well defined threshold has been reached[18]. This is the basis for some display devices. There are two important differences: in nematics, flows are only transient, and the distortion sets in because of the action of an external orienting field. In active polar systems the distortion arises spontaneously without any externally orienting field and permanent flow results. Yet instability conditions, the polarization distortion and flow field above threshold can be calculated in a way fairly similar to that of the Frederiks transition[23]. The activity threshold reads:

$$\zeta\Delta\mu_c = \frac{\pi^2 K(4\eta/\gamma_1 + (\nu_1+1)^2)}{-2L^2(\nu_1+1)}. \tag{10}$$

The minus sign shows that the instability exists only if the gel is contractile. L is the thickness of the slab and the other coefficients are defined in Eq.(6). The threshold value tends to zero for large enough thickness, at constant contractility: infinite size homogeneous active gels do not exist. There is always an instability, which can be at finite wave vector depending on boundary conditions for large enough systems. The stability of fluctuating modes have been worked out, for thin and bulk compressible systems [21, 24, 25].

Note that we have discussed here a simple shear since it is rather easy to realize in the lab. A pure elongational shear orients the nematic director either parallel or perpendicular to it. This geometry cannot be obtained in any clean way with liquid crystals: we will show in section 6 that it occurs spontaneously in biological systems and that it is physiologically important.

Topological singularities provide nice signatures of the of the phase symmetries. It is thus natural to characterize the topological singularities of active gels. In nematic liquid crystals such singularities are called disclinations. They can be classified with homotopy groups [26]. Defining a contour around the singularity point one counts the number of angular rotations of the nematic director, obtained in one rotation around the contour it can be integer or half-integer. For polar nematics, this number is necessarily an integer, positive if the rotation of the polar vector is in the sense of the contour and negative if it is in the opposite sense. It is called the strength of the disclination. We give on 3 the three possibilities corresponding to disclinations of strength one. Since active gels behave like active polar nematics on long time scales, one expects the same geometrical aspects for the disclinations. However, the temporal symmetry is different: equilibrium systems are invariant upon time reversal (changing

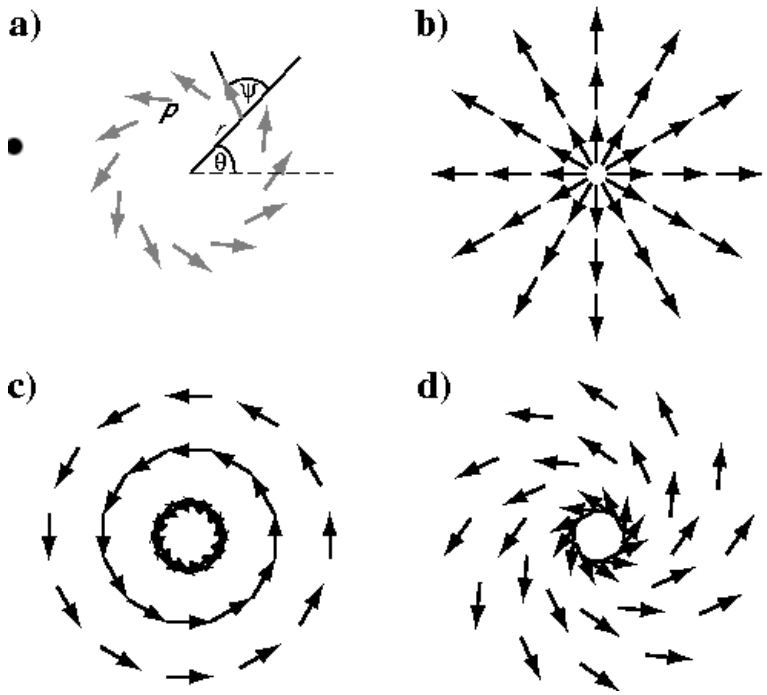

Figure 3: Disclinations of strength one in polar nematics. a)Definition of the angles.b)Stable structure when $K_1 < K_3$.c)Stable structure when $K_1 > K_3$.d)When $K_1 = K_3$ all spirals with indeterminateψ are are stable.From Ref. [14].

t in $-t$), whereas active systems are not. On general grounds one expects thus, differences in the dynamical behavior of the disclinations. The case d) of (3) is particularly interesting: the spatial symmetry is such that the positive and negative rotations are not equivalent. Combined with the absence of time reversal symmetry, one concludes that such spirals should rotate permanently. Eqs.(6), (7) can be solved analytically, if we chose boundary conditions such that at a radius R from the singularity center, the angle ψ takes on the value such that $cos(2\psi_0) = \frac{1}{\nu_1}$. Indeed, we expect a shear flow to exist and thus the flow alignment to impose this orientation in the bulk of the disclination, breaking the passive degeneracy. Choosing the same orientation at the boundary, suppresses the boundary layer and leads to simple results.

With these values of ψ_0, we find for the shear rate $u_{r\theta}$:

$$u_{r\theta} = \frac{\sin 2\psi_0}{4\eta + \gamma_1 \nu_1^2 \sin^2 2\psi_0} \tilde{\zeta} \Delta\mu \quad . \tag{11}$$

The velocity is ortho-radial, along the θ direction; it is obtained from (11)

$$v_\theta \;=\; 2r \left(\int_0^r \frac{u_{r\theta}}{r'} dr' + v_\theta^0 \right) \tag{12}$$

where v_θ^0 is an integration constant. For a finite system with radius R

and with the boundary condition that no motion occurs at the boundary,

$$v_\theta = 2u_{r\theta} r \log \frac{r}{R} \quad . \tag{13}$$

In the cases a) and b) for "small" $\zeta\Delta\mu$, we find that there is no motion. Strictly speaking this result holds for the barycentric velocity only. The absence of motion is obvious for case a). For case c) there are constant fluxes indicating rotating motion for instance of the motors around the singularity center, the term describing them appears in the densities conservation equations. For larger $\zeta\Delta\mu$, beyond a critical value depending on the elastic moduli anisotropy $K_1 - K_3$, we find that the immobile disclinations become unstable with respect to the onset of a rotating state [14, 15]. Strength one disclinations of type b), c), and d) are called respectively asters, vortices and spirals. Biological systems which follow the general definition of active gel, have shown the existence of both immobile asters and rotating spirals [7]. A detailed comparison with our results cannot be made though, because the experiments do not correspond to the long wavelength limit. Eventually, the existence of moving spirals provides a paradigm for what is called low Reynolds Number turbulence [5, 24, 21].

4 Cell Motility

In section 2 we have derived generic hydrodynamic equations for active gels and in section 3 we have discussed simple experimental situations which except for the last one, have a priori little connection with Biology. In this section we discuss some features of a Keratocyte lamellipodium. Fish keratocytes are eukaryotic cells which can easily be obtained by pulling out a fish scale and dipping it in an appropriate physiological serum. If one squeezes a drop of the obtained suspension under a microscope, one observes after sedimentation, cells moving steadily on the lower coverslip. The velocity is of the order of $10\mu/min$, which for a cell is fast. The reason for this high speed is probably the function of keratocyte cells in wound healing: they dash to the wound. They draw a sizable attention because their motion is steady and their shape is smooth and invariant during the motion: it looks like a good start for understanding cell motility. The top image that one sees on Fig (4) shows a keratocyte moving upwards. Aside from the nucleus which builds a protuberance of the order of ten microns in the central rear region of the cell, the rest is fairly thin, of the order of a micron or less. The flat region in front of the nucleus is called the lamellipodium (sometimes the lamella), it extends from the leading edge to the vicinity of the nucleus. This region is filled with an actin gel, cross-linked by several proteins or protein complexes which are displayed on the middle and bottom of the Fig (4). Since the cross-links have a finite life time (of order tens of seconds), it is a physical gel. In addition, myosin motor bundles can grab two filaments at a time and exert a stress on the structure. Since the motor activity requires ATP hydrolysis the lamellipodium acto-myosin system obeys exactly our definition of an active gel.

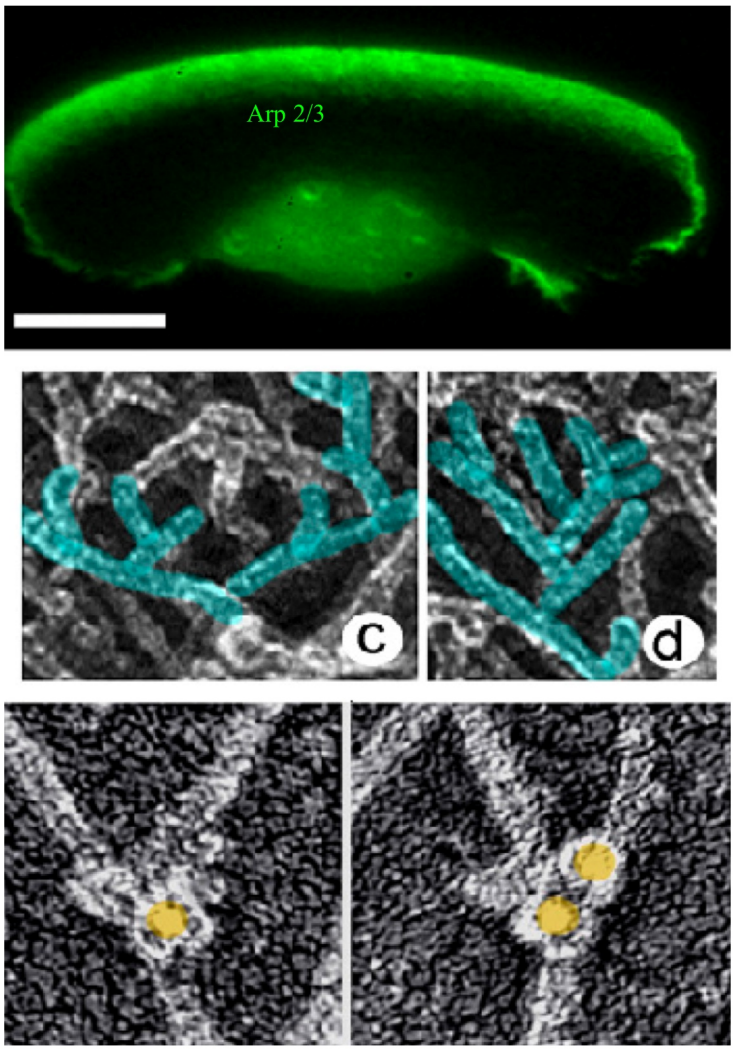

Figure 4: Top image:keratocyte crawling on a substrate towards the top of the image.Bar=5μ. Middle images: actin network viewed with electron microscopy (the width of the filaments is 5 nanometers). Bottom image: close up view on a protein complex (Arp2/Arp3) known to play an important role in the assembling process of the network. [17].

The biochemistry involved in the motion is well documented. We give here a minimal description. At the leading edge or very close to it, the actin network is assembled by polymerization and cross-linking. Further into the cell, in the vicinity of the nucleus actin depolymerizes. This process is also typically out of equilibrium. The assembling units are ATP actin monomers, whereas the disassembling ones are ADP monomers: the filaments have been hydrolyzed along the way. It is known from molecular biology, that this polymerization/depolymerization process is the main mechanism responsible for motion. This is not true of all types of motility, for instance it does not hold for ameoboid motion.

Ideally one would like to be able to describe the three dimensional

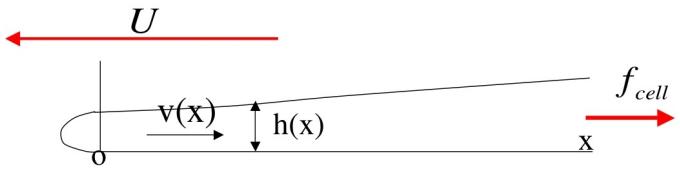

Figure 5: Sketch of an advancing lamellipodium.

cell shape, how it relates to speed and what is its response to external forces. We are not yet able to achieve such a task. We will just describe the lamellipodium profile perpendicular to the leading edge, in the central region of the keratocyte. In this region, in general, the leading edge is fairly straight and one can consider that the problem is translationally invariant in the direction parallel to the leading edge. A typical shape is sketched on Fig.5. The lamellipodium moves globally to the left with velocity U keeping its shape constant. By definition U is taken to be positive. The gel moves with respect to the substrate with velocity $\mathbf{v}$, it is essentially oriented along the x direction. We call v this x component omitting the subscript; it is positive if the gel motion is to the right. To find the motion characteristics and the shape of the lamellipodium, we must solve Eqs.6, 7, with appropriate boundary conditions, keeping track of the polymerization process at the leading edge and of the interaction between the gel and the phospholipid membrane which envelopes the cell (plasma membrane). We take as an experimental input the fact that the filament orientation does not seem to vary significantly in these regions of the lamellipodium. We thus take $\mathbf{p}$ parallel to the x direction everywhere which solves Eq. 7 trivially. We treat separately a proximal region where the membrane is not in contact with the substrate (i.e. to the left of the origin labeled O), and a distal one where it is in contact with the substrate (to the right of the origin).

4.1 Proximal region

In this region, the main challenge is to describe the interaction of the polymerizing gel and the plasma membrane [27]. The gel velocity field varies over a length scale which is larger than that of the proximal region: thus it can safely be considered as constant there. Once we have described the interaction with the membrane, all we have to do is match, the velocity field and conserve forces in the plane of the origin O.

The velocities that we are considering are tens of microns per minute and for steady state shapes, the hydrodynamic forces on the membrane are totally negligible. Thus for all practical purposes the membrane is in mechanical equilibrium:

$$0 = \frac{\delta F^{tot}}{\delta r_n}. \tag{14}$$

For a fluid membrane, the variation has to be taken with respect to displacements r_n normal to it. F^{tot} is the sum of the energy of the bare

membrane F_m and the gel-membrane interaction energy. Its variation is easy to express in terms of the gel stress normal to the membrane and the bare membrane free energy:

$$\delta F^{tot} = \delta F_m + \int ds \delta r_n (\sigma_{n,n} - \delta P) \ . \tag{15}$$

In this equation, the variations are taken again with respect to displacements δr_n; $\sigma_{n,n}$ is the normal-normal component of the gel stress tensor and δP the hydrostatic pressure difference between interior and exterior of the cell and ds the surface element on the membrane. The membrane bare free energy is that of a membrane under tension, with curvature rigidity and possibly spontaneous curvature as first introduced by Helfrich [28]:

$$F_m = \int ds (\sigma + \frac{K}{2} (\frac{d\theta}{ds} - C_0)^2) \ . \tag{16}$$

The question of the membrane shape at the tip is a well posed problem if one knows $\sigma_{n,n}$. The way it enters Eq. 15 shows that it provides an effective pressure difference. $\sigma_{n,n}$ can be obtained in an implicit way, by imposing that the polymerization rate parallel to the x direction must lead to a uniform displacement of the structure with velocity U to the left. Indeed the polymerization rate V_p is a function of the stress $V_p(\sigma_{n,n})$, and the continuity of the structure requires:

$$V_p(\sigma_{n,n}) = U + v \ . \tag{17}$$

Thus for a given U, extracting v from our hydrodynamic equations one can invert Eq.17 to obtain $\sigma_{n,n}$. Microscopic theories relating polymerization rate and stress come into this relation [29, 30]. It is important to understand that the stress value depends on v which involves solving the hydrodynamic equations in the distal region: the effective pressure exerted by the polymerizing gel is not a local property. One can illustrate the argument further by considering a "small" stress regime:

$$V_p(\sigma_{n,n}) = V_{p0} + \lambda \sigma_{n,n} \ . \tag{18}$$

The effective pressure then reads:

$$\delta P^{eff} = \delta P + \frac{V_{p0} - (v + U)}{\lambda} \ . \tag{19}$$

The shape of a membrane submitted to a pressure difference is a well known problem. One can immediately infers that provided the length $\sqrt{(\frac{K}{\sigma})}$ is small compared to the lamellipodium thickness the radius of curvature at the leading edge is given by Laplace's law $R_l = \frac{\sigma}{\delta P^{eff}}$ and that the global shape is as sketched on Fig.5. Conversely, taking the curvature radius of the order of the thickness and typical membrane tension values, we can estimate the value of the effective pressure to be of the order of 10^3Pa.

Force balance imposes that the integrated effective pressure difference matches exactly the pulling forces due to membrane tension together

with external forces applied in the proximal region:

$$P^{eff}h(x=0) = \sigma + \sigma\prime + f_p^{ext} \tag{20}$$

σ is the tension of the membrane in the presence of the gel as already introduced and $\sigma\prime$ is the tension "dressed" by the interaction of the membrane with the substrate. It could be negative and help the motion if the membrane tends to wet the substrate. f_p^{ext} is the integrated external force on the proximal region. Replacing P^{eff} by its expression Eq. 19 one can express the polymerization velocity as a function of applied force and membrane tensions:

$$V_p = U + v = V_{p0} - \lambda \frac{\sigma + \sigma\prime + f_p^{ext}}{h(x=0)} \ . \tag{21}$$

This expression shows that for a given tension there is a minimum thickness below which lamellipodia cannot grow. One sees also that an external force can either speed up or halt polymerization at constant thickness. In order to get a complete picture, we now need to calculate the gel velocity field v and the height profile h in the distal region.

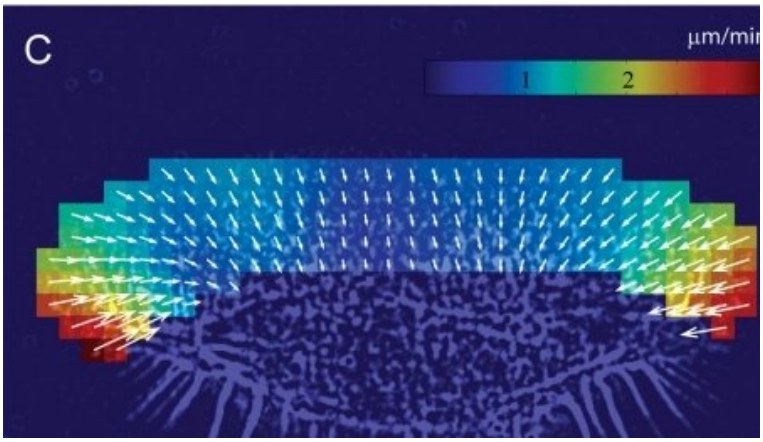

Figure 6: Velocity field determined by speckle microscopy in a lamellipodium. Figure from Ref. [31]

.

4.2 Distal region

The gel dynamics is ruled by Eq. 6. Taking as boundary condition that both the normal and tangential stresses must vanish at the free surface of the lamellipodium, in a lubrication approximation we can recast the equation in a form involving only the thickness averaged velocity field $h(x)v(x) = \int dz v(x,z)$ and the force $f(x) = \int dz \sigma_{x,x}(x,z)$:

$$4\eta \frac{dv}{dx} = (1 + \tau U \frac{d}{dx}) \frac{f}{h} + \zeta \Delta\mu \ . \tag{22}$$

An important point concerns the dynamical interaction of the gel and the substrate. The actin network is connected to the substrate by binding

proteins. One could believe that the correct boundary condition is a no slip boundary condition. This is not the correct choice, because the bound state has a finite lifetime. For the slow motion we consider, the average force transmitted to the substrate can be shown to be proportional to the slip velocity [32, 33]. For large rates on can reach stick-slip regimes which have been observed in the Listeria motility [32], this last regime may correspond to fibroblast motion and in some cases to keratocytes but most of time a linear friction is sufficient. Expressing the global conservation of force reads:

$$\frac{df}{dx} = \xi v \ . \tag{23}$$

Eventually, global volume conservation leads to the relation:

$$h(x)(U + v(x)) = const \ . \tag{24}$$

With proper boundary conditions this set of equations is complete and can provide both the gel velocity field and the height profile. At the origin, one has to match distal and proximal solutions. In particular, forces must be conserved. At the rear of the lamellipodium, which we will also call the trailing edge the boundary conditions are less well defined. The depolymerization process being rather well localized in space we take as a first attempt a depolymerization occuring in a well defined plane $x = L$. In the case of cell fragments, we have discussed spatially distributed depolymerization [34], but for the case at hand, this simplification will be sufficient. At the trailing edge $x = L$ forces must be matched. We call f_L^{ext} the force that the rest of the cell is exerting on the lamellipodium (a genuine external force could be added as well). With these "rules" everything can be calculated [35]. One can get further insight by noting that the thickness variations are small. If on linearizes the equations around the average thickness $\bar{h}$, one can solve the equations analytically. An important point, comes from the comparison of Eqs.22 and 23: eliminating the velocity in 22 with its value obtained from 23 one sees the emergence of the length scale $d = \sqrt{\frac{2\eta\bar{h}}{\xi}}$. Forces and velocities are screened over a length scale d. In the regime where $L \gg d$ we find:

$$f(x) = (\zeta\Delta\mu\bar{h} - (\sigma+\sigma\prime) + \xi\tau v(0)(U + v(0) - f_p^{ext}) \exp(-\frac{x}{d} + (f_L^{ext} + \zeta\Delta\mu\bar{h}) \exp(\frac{x-L}{d}) - \zeta\Delta\mu\bar{h} \tag{25}$$

and

$$v(x) = \frac{1}{\xi d}(-(\zeta\Delta\mu\bar{h} - (\sigma+\sigma\prime) + \xi\tau v(0)(U + v(0) - f_p^{ext}) \exp(-\frac{x}{d} + (f_L^{ext} + \zeta\Delta\mu\bar{h}) \exp(\frac{x-L}{d})) \tag{26}$$

with

$$v(0) \simeq \frac{-\zeta\Delta\mu\bar{h} + (\sigma + \sigma\prime) + f_p^{ext}}{\xi(d + \tau U)} \tag{27}$$

and

$$v(L) \simeq \frac{f_L^{ext} + \zeta \Delta\mu \bar{h}}{\xi d} \tag{28}$$

and eventually

$$U = v_{dp} - v(L) \simeq v_{dp}(f_L^{ext}) - \frac{f_L^{ext} + \zeta \Delta\mu \bar{h}}{\xi d} \ . \tag{29}$$

In this last equation v_{dp} is the depolymerization velocity. It can depend on stress but not on monomer concentration. The values of the gel velocities at the leading edge and at the trailing edge are completely decoupled. Note that $v(0)$ in the absence of external force is positive since $\zeta\Delta\mu$ is negative and the tensions sum is in general positive. Thus, even though the motion of the lamellipodium is to the left, the gel moves to the right: this motion called retrograde motion is indeed found by biologists (Fig.6)[31]. The measured profiles of both velocity and force exerted on the substrate can be compared to the resuts of Eqs.(26, 25), in the case when there is no applied force at the leading edge $f_p^{ext} = 0$, and the force at L is entirely due to the cell $f_L^{ext} = f^{cell}$. One can extract both the contractility and the friction coefficients. One finds for the contractility $\zeta\Delta\mu \simeq -10^3 Pa$ and for the substrate friction $\xi \simeq 310^1 0 Pa$. The contractility is about one tenth of the short time shear modulus and the friction is of the same order of magnitude as that found experimentally in vitro for a passive actin gel/polystyrene interface [36].

Note that the steady state velocity U depends on the external force at the trailing edge f_L^{ext} but not on the force at the leading edge. This may seem surprising at first sight, but results from the steady state conditions. The predicted effect of forces is non trivial and results from the fact that at steady state monomer conservation imposes $h(0)V_p = h(L)V_{dp}$. Since the polymerization rate $v_p = k_p C(0)$ depends on the actin monomer concentration at the leading edge $C(0)$, and the monomers diffuse from the cell body to the leading edge, the length of the lamellipodium adjusts in such a way that the monomer concentration drops enough for the former equality to hold. It is thus the depolymerization rate which fixes the speed.

Suppose first that, starting from steady state, we turn on and maintain a force opposing the motion f_L^{ext} at the trailing edge. The explicit dependence of U on f_L^{ext} suggests that one should observe a slowing down of the lamellipodium. This will hold if v_{dp} does not depend on force. However, biochemistry, tells us that v_{dp} should increase exponentially with f_L^{ext}. Then applying an opposing force at the trailing edge could result in a speeding of the lamellipodium, at steady state!

Suppose now that, starting from a steady state we turn on a force f_p^{ext} opposing the motion and which we maintain constant. The leading edge naturally slows down (k_p decreases), but as it slows down the length L of the lamellipodium decreases and the actin monomer concentration increases. This process goes on until the concentration is high enough for the steady state to be restored. For not too large forces, the inequality

$L >> d$ still holds and U is still given by Eq. 29! If the force is larger, one may get to a regime where $L < d$, in which the gel velocity is constant:

$$v \simeq \frac{1}{xi(L+\tau U)}(f_L^{ext} + f_p^{ext} + \sigma + \sigma\prime) \tag{30}$$

and the lamellipodium velocity now depends on all forces:

$$U \simeq v_{dp} - \frac{1}{\xi(L+\tau U)}(f_L^{ext} + f_p^{ext} + \sigma + \sigma\prime) \ . \tag{31}$$

Thus the predicted response of a lamellipodium to an opposing force applied at the leading edge is that the lamellipodium first shrinks without slowing down and only when it is "small" it does slow down.

5 Cell Oscillations

There are several instances where the shape of a cell shows periodic oscillations. When the microtubules in a cell are depolymerized using a drug, the cell oscillates by forming a bleb which is a protrusion where the membrane is detached from the cytoskeleton [37]. Due to the contractility of the cortical actin layer in the cell body, the pressure in the cell body is larger than that in the bleb and the cytoplasm flows into the bleb. In an oscillating cell, the bleb is unstable and the whole cytoplasm empties in the bleb. The cortical layer then repolymerizes and the oscillation occurs by successive formation of unstable blebs. An example of oscillating cell is shown in Fig.7. The period of the oscillation is of the order of 10 minutes and the oscillation disappears when either actin or myosins are inhibited which is a clear indication that the contractility of the cortical layer drives the oscillation. Cell fragments which are formed by extraction of the nucleus show similar oscillations with a smaller period of the order of 2 minutes. These oscillations has been observed with several cell types.

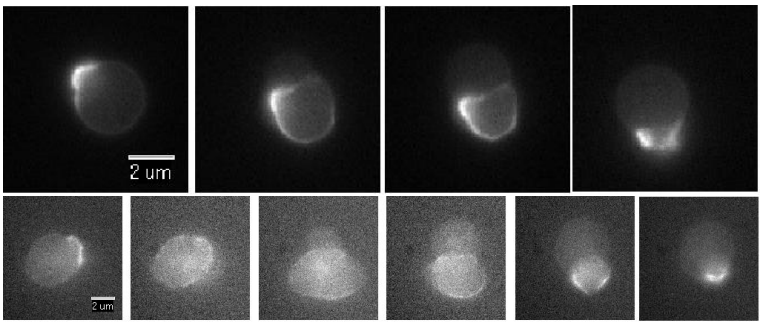

Figure 7: Shape oscillations after microtubule depolymerization of mice fibroblasts: in the first frame actin is fluorescently labeled; in the second frame myosin is fluorescently labeled. The labeling clearly shows the cortical layer in the cell body and the growth of a bleb which has no cortical layer and which invades the whole cell. After one oscillation, a new bleb appears Courtesy C. Sykes, E.Paluch

Another type of shape oscillations is observed for fibroblast cells floating in solution when adhesion on any surface is prevented as shown

on Fig.8 [38]. The period of the oscillation is very well defined and of the order of 30s. As in the previous example, disruption of the cortical actin layer and inhibition of the myosin stops the oscillation. Myosin activity in a cell can be modulated by introducing various drugs. These experiments show that the oscillation period decreases when myosin activity increases. Another key component for the oscillation is the presence of extracellular calcium. The oscillation disappears if the medium is depleted in calcium. This suggests that calcium channels play an important role. Although the nature of calcium channels in these cells is not known, the addition of an inhibitor of ion channels stops the oscillations. Similar oscillations have been observed after depolymerization of the microtubules in Ref.[39]

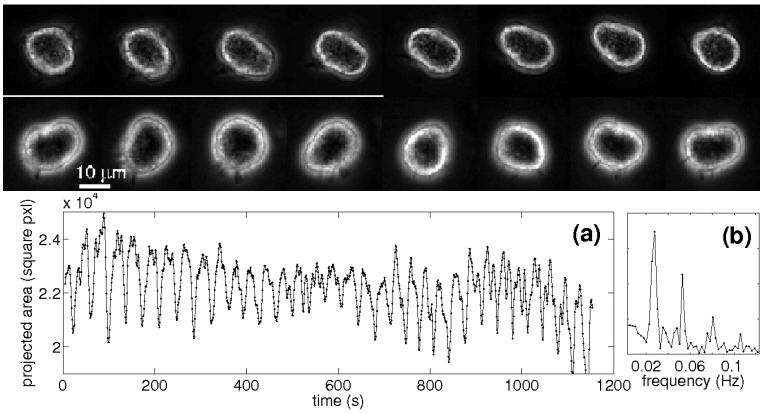

Figure 8: Shape oscillations of non-adhering fibroblasts. The second frame shows the periodic oscillation of the projected area of the cell and the associated Fourier spectrum. Figure from Ref.[38]

In order to study the oscillations of suspended cells we assume that the membrane in these cells contains calcium channels and that these channels are gated by the deformation of the actin cortical layer x defined as the relative change in local area of the cortical layer [38]. If the deformation is large, the channels are open and if the deformation is small the channels are closed. For an incompressible layer of thickness e any change in the deformation is related to a relative change in thickness $\delta x = -\delta e/e$. The precize mathematical form of the opening probability $p_o(x)$ of the channels is not known but it is a sigmoidal function varying between 0 and 1 with a sharp variation around a critical value x_c that we suppose to be small.

When calcium enters the cell, it undergoes a cascade of chemical reactions with calmodulin and the myosin light chain kinase which eventually leads to a phosphorylation of the myosins light chains and an increase in activity. A detailed study of the chemical reactions involved leads to a variation of the free calcium concentration in the cell as

$$\frac{d[Ca]}{dt} = \left[-k_{[Ca]}([Ca] - [Ca]_{cell}) + \lambda p_0(x)\right] \ . \tag{32}$$

The first term describes the effect of calcium pumps which tend to drive the concentration back to its equilibrium value $[Ca]_{cell}$ and the second

term describe calcium penetration through the channel; the coefficient λ is proportional to the difference of the calcium chemical potentials inside and outside the cell and therefore depends on the calcium concentration in the external medium. We will assume here that the calcium concentration in the cell is not uniform and that the local opening of the calcium channels only modifies the local calcium concentration. This is justified by the fact that most of the calcium in the cell is sequestered by calmodulin and diffuses very slowly.

For the sake of simplicity, we assume that a small change in the calcium concentration $\delta[Ca]$ induces a small change in the local myosin activity $\delta\zeta\Delta\mu$ proportional to $\delta[Ca]$. This leads to an equation for the local variation of the myosin activity of the form

$$\frac{d(\delta\zeta\Delta\mu)}{dt} = -k_{[Ca]}\delta\zeta\Delta\mu - k_f\delta e/e \tag{33}$$

where k_f is a retroaction coefficient proportional to both λ and to the variation of the opening probability with the deformation $\frac{dp_o(x)}{dx}$.

The mechanism of the instability is sketched on Fig.9. If the cortical layer is stretched on one side of the cell and compressed on the other one, the calcium channels are open on the side where the membrane is stretched and calcium enters the cell on this side. The local increase of contractility provokes a local compression of the cortical layer and a closure of the channels. On the opposite side, the cortex is stretched and the channels open. The oscillation can then proceed.

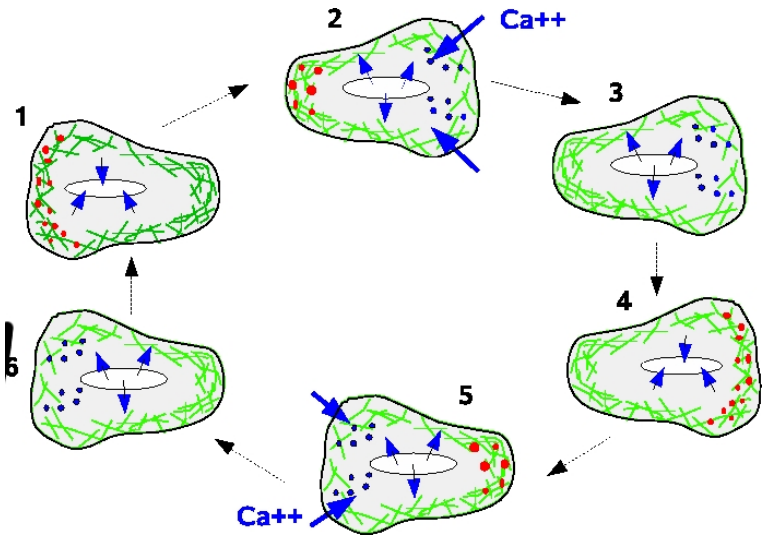

Figure 9: Sketch of the oscillation mechanism. Figure from Ref.[38]

The change in the cortical layer thickness is due both to a lateral flow of actin along the cortical layer and to the constant polymerization and depolymerization of the filaments (the so-called treadmilling process). We study the instability here ignoring treadmilling that we consider as very slow and we only consider the lateral actin flow. This flow obeys

Eqs. 9,6 since the cortical actin network obeys again our definition of an active gel. It is similar to the lamellipodium gel, but different in that the filament directions are on average parallel to the plasma membrane and thus perpendicular to the local symmetry axis, which is also the **p** axis. As a result, the gel is contractile in the plane parallel to the membrane.

In the absence of interaction with a substrate, cells are on average spherical. Thus we consider a spherical cell and perform a linear perturbation analysis expanding the shape in Legendre polynomials (assuming azimuthal symmetry). It turns out that the most unstable mode always corresponds to a Legendre Polynomial $n = 1$. This mode is somewhat peculiar since a perturbation of a sphere with a mode $n = 1$ gives a translation of the sphere. The radius of the cell R is therefore not changed by such a perturbation. The thickness of the cortical layer e however is proportional to $\cos\theta$ corresponding to a thinning of the cortical layer at one pole and a thickening at the other pole. The amplitude of the $n = 1$ mode for the thickness of the cortical layer can be calculated from the active gel theory. This leads to

$$\tau \frac{d\delta e/e}{dt} = \frac{\zeta \Delta\mu}{6E}\delta e/e + (1 + \tau\frac{d}{dt})\frac{\delta\zeta\Delta\mu}{6E} \tag{34}$$

The stability of the cortical layer can be studied from the dynamical system formed by Eq.33, 34. The results are summarized in the stability diagram of Fig.10. There are three regions in this diagram. At low

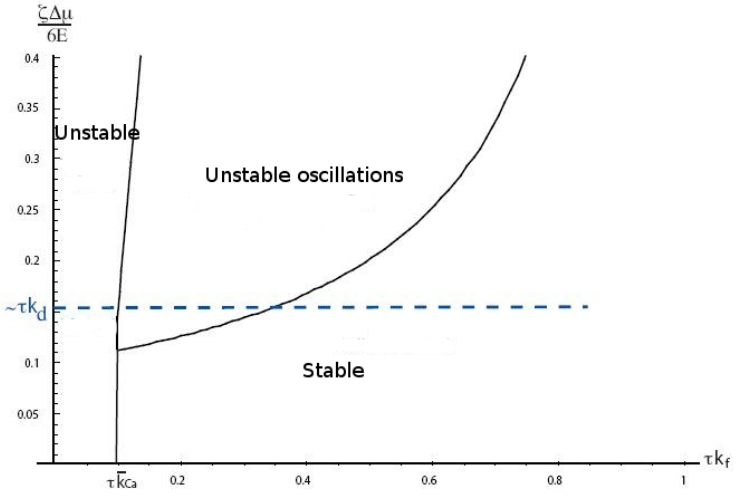

Figure 10: Stability diagram for a non adhering cell. The vertical axis is proportional to the activity and the horizontal axis to $k_f\tau$ where k_f is the retroaction coefficient associated to the channels and τ the Maxwell viscoelastic relaxation time

activity and large enough value of $k_f\tau$ the spherical cell shape is stable. At small values of $k_f\tau$, the cell is unstable but there is no oscillation. As the instability grows the thickness decreases on one side of the cell and eventually a hole forms in the cortex. In this range of parameters, one expects either the blebbing oscillations of Paluch et al. or the apparition

of blebs. In the central region of the stability diagram, the cell is unstable with respect to an oscillatory mode with the symmetry of a mode $n = 1$. The shape of the cell does not change in the linearized theory that we present here. However if the prameters are not too close to the instability threshold, there are couplings between the $n = 1$ mode and higher order modes which could lead to an oscillation of the cell shape. The period of the oscillations is given by

$$\tau_{osc} = \frac{2\pi\tau}{\sqrt{\frac{\zeta\delta\mu}{6E}(4\tau k_f - (1-\tau k_f)^2\frac{\zeta\delta\mu}{3E})}} \ . \tag{35}$$

As shown on Fig.11 the period decreases with the activity as observed experimentally. Finally the horizontal line on Fig.10 corresponds to the

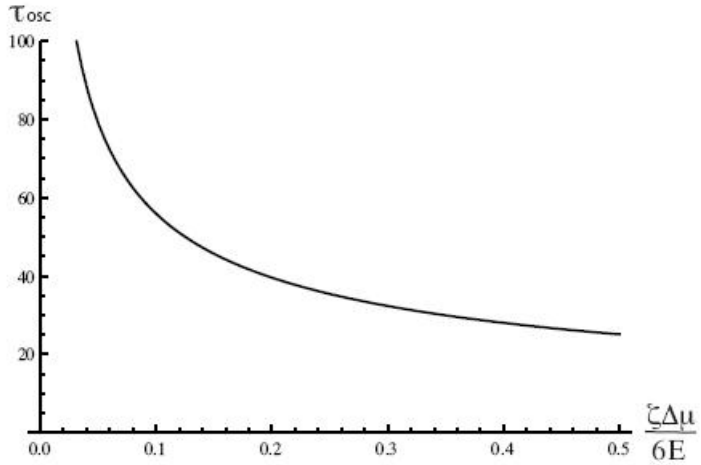

Figure 11: Variation of the oscillation period with the myosin activity

limit of validity of the theory. If the activity is smaller than $E\tau k_f$, treadmilling is important and stabilizes the cortical layer.

6 Wound Healing and Cytokinesis

Cell division proceeds by successive steps. In a first step, the S phase, the cell duplicates its biological material. During mitosis, the chromosomes of the two daughter cells separate and form two nuclei precursor to the two daughter cells [2]. After mitosis the two cells separate in a process called cytokinesis. At the beginning of mitosis the cells are roughly spherical: the actin cortical layer discussed in the previous section recruits myosin motors and becomes more active leading to an increase of the cortical tension. After mitosis, the activity of the cortical layer is non-homogeneous, there is an excess of myosins at the equator of the cell and the activity is larger at the equator than at the poles [40]. The gradient in activity drives a cortical flow from the pole to the equator, which has recently been experimentally studied in details[41]. When the flow develops, an

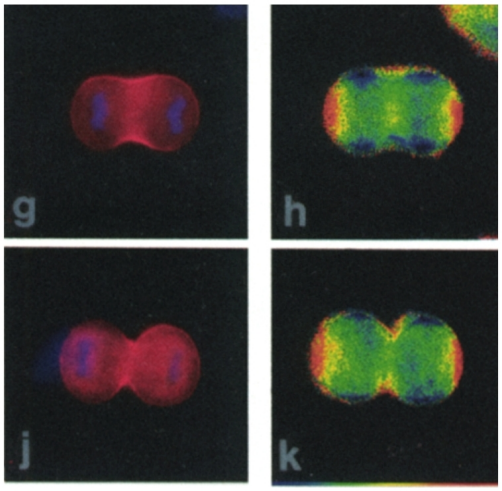

Figure 12: Cytokinesis and formation of the cleavage furrow. On the left pannel the cell nuclei are labeled in blue. On the right pannel, the actin filaments are labeled in blue, red or yellow. A blue or red color corresponds to an orientation of the filaments from the pole to the equator and a yellow color to an orientation around the equator. Figure from Ref.[42]

actin ring appears along the equator as shown on Fig.12 [42]. The ring is contractile and pinches the cell to create a so-called cleavage furrow. Eventually the cleavage furrow shrinks and leads to the formation of a bridge and to the separation of the two daughter cells when the bridge ruptures.

The aim of this section is to study quantitatively the apparition of the cortical flow and the formation of the contractile ring appearing during cytokinesis. There are several instances in cellular biology where contractile rings form. A spectacular example is that of wound healing in a xenopus embryo. The authors of ref.[43] make a wound in a xenopus embryo by laser ablation. As shown on Fig.13, the wound is a circular hole in the cortex with a size of the order of 50μm. Just after the wound formation, myosins are recruited around the hole in a rim with a width of the order of 5μm. There is thus in this rim an increase in activity [44]. As for cytokinesis, the gradient in activity induces a flow towards the rim which heals the wound at a constant radial velocity of the order of $0.04\mu m/s$. Before the wound formation the actin filaments in the cortical layer are randomly oriented in the tangent plane to the embryo. When the wound heals, the actin filaments are oriented radially towards the center of the wound outside the rim of increased activity and tangent to the wound edge inside the rim. They thus form a contractile ring around the wound. Another similarity with cytokinesis is that the recruitment of myosin motors around the wound is independent of actin but it seems rather due to an increase of microtubule concentration around the wound. Other contractile rings are observed during the first division of C.Elegans embryos or in the dorsal closure of drosophila. In this last case the actin

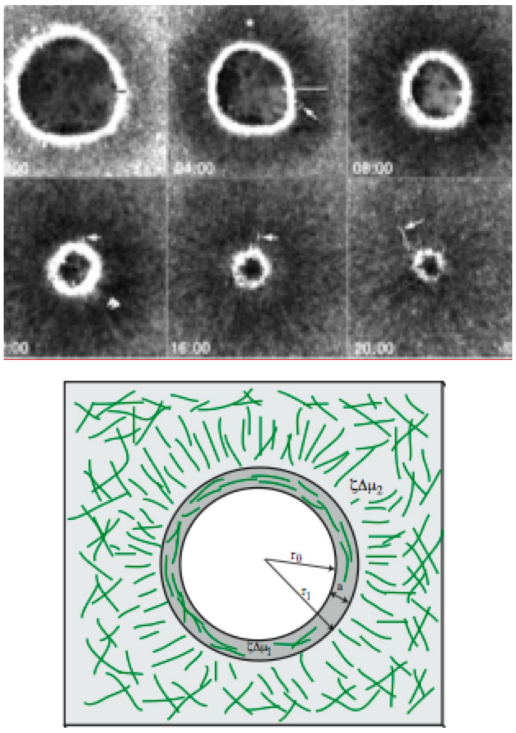

Figure 13: Wound healing in a xenopus embryo. Upper figure: time laps picture of wound healing after hole punching in a xenopus embryo cortex. Figure from Ref.[44]. Lower figure: schematic representation of the actin filaments distribution, and definition of the symbols used in the text. Figure from Ref.[38]

ring is not observed in a single cell but rather in a tissue. It spans over all the cells surrounding the closing hole.

The geometry of wound healing in xenopus embryos which is almost planar with a rotational symmetry is far simpler that that of the dividing cells. We therefore first discuss wound healing and then present very briefly our results on cytokinesis [45]. The closure of the wound is due to a competition between the contractile active stress away form the wound which tends to open the hole and the increased activity in the rim around the wound which tends to close the wound. In the absence of increased activity around the hole, the group of F. Brochard [46] has shown that a hole in a visco-elastic film opens with a radius increasing exponentially with time. The increased activity in the rim increases locally the cortical tension and the local increase of the cortical tension drives the closure of the wound. In order to use the active gel theory for a film with randomly oriented filaments, it first must be generalized to systems with pretransitional nematic order. The nematic order parameter is defined in two dimensions as $Q_{ij} = \langle n_i n_j - \delta_{ij}/2 \rangle$ where n_i is the ith component of the local orientation of the actin filament. It is a traceless tensor and in a system with rotational symmetry it has a single independent parameter $\tilde{Q}$ which is positive if the actin filaments are pointing radially towards the center of the wound and negative if the actin filaments are pointing

tangentially around the wound. In polar coordinates, the generalization of the active gel theory to gels in two dimensions with a nematic order leads to the two following equations for the order parameter $\tilde{Q}$ and the radial velocity v_r.

$$\begin{aligned} 4\eta\partial_r(\partial_r + \frac{1}{r})v_r &+ (\partial_r + \frac{2}{r})(\zeta\Delta\mu + \beta_1\chi)\tilde{Q} = 0 \\ \frac{\partial\tilde{Q}}{\partial t} &= -\frac{\chi}{\beta_2}\tilde{Q} + \frac{\beta_1}{2}(\partial_r - \frac{1}{r})v_r \ . \end{aligned} \tag{36}$$

The first equation is the force balance equation and the second equation is the equation for the relaxation of the order parameter.The first term on the left hand side of the force balance equation is the gradient of the viscous stress, the second term is due to the gradient of the active stress where in this section the activity coefficient ζ is positive and the last term is the coupling to the order parameter. As already mentioned, contractility is in the plane of the cortex and perpendicular to the polarization axis. The reactive coefficient β_1 is related to the coupling coefficient ν_1 introduced in Eq.6 by $\nu_1 = -\beta_1/S + o(1/S)$ where S is the nematic order parameter. The sign of β_1 is not imposed by the theory. We only consider here the case where β_1 is positive which corresponds to an orientation of the actin filaments in the direction of an elongation (i.e. that of a positive velocity gradient). The nematic susceptibility χ is positive. In the second equation, the dissipative coefficient β_2 is positive and it is related to the rotational viscosity by $\gamma_1 = 2\beta_2 S$.

We consider now the wound as a circular hole in the cortex of a xenopus embryo with a radius r_0. In the rim of size $a = r_1 - r_0$ around the wound where the myosins are recruited, the active stress is $\zeta_1\Delta\mu$. Outside the rim, the myosin density is lower and the active stress is $\zeta\Delta\mu$ with $\zeta_1 > \zeta$. The dynamic equations can be solved easily in the limit where the relaxation of the order parameter is fast i.e. in the limit where the $\frac{\partial\tilde{Q}}{\partial t}$ term is negligible in Eq.36. The hole closes only if the activity is large enough namely when $\zeta\Delta\mu_1 > \left(\frac{8\zeta\Delta\mu\eta\chi r_0}{a\beta_1\beta_2}\right)^{1/2}$. Above the threshold activity, we give in Fig.14 a plot of both the order parameter and the radial velocity v_r.

Outside the rim $r > r_1$, the velocity modulus obtained from Eq. 36 decreases with increasing r as $1/r$ faster than the observed velocity which decays exponentially to zero. This is accounted for in Fig.14 by adding in the equation of motion 36 a viscous friction between the cortex and the membrane. Outside the rim, the velocity gradient drives the order parameter $\tilde{Q}$ to a positive value corresponding to a radial orientation of the filaments. The gradient in the active stress drives thus a radial flow which itself orients the actin filaments. Inside the rim $r_0 < r < r_1$, the velocity gradient has the opposite sign, the order parameter is negative and the actin filaments are oriented in the tangential direction. The velocity modulus decreases with decreasing r and the maximal velocity is reached at the edge of the rim $r = r_1$. The variation of the radius of the wound r_0 is equal to the velocity at r_0. If we assume as seems to be the

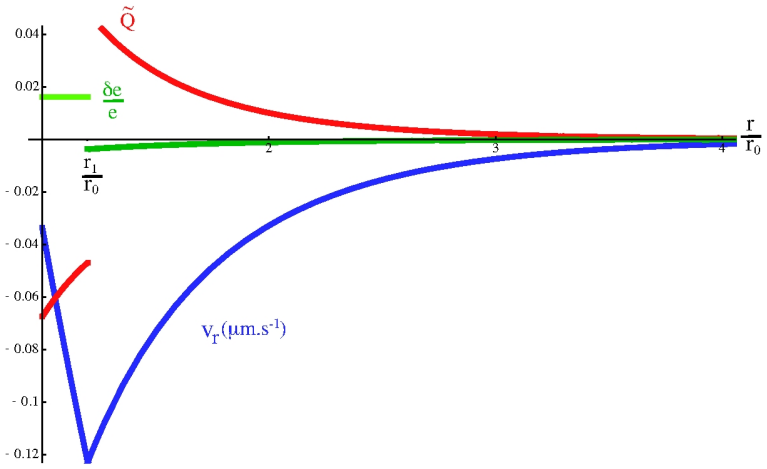

Figure 14: Radial actin velocity (blue curve) and nematic order parameter (red curve) during the wound healing of a xenopus embryo

case experimentally that the size of the active rim a is constant, we find a constant closing velocity

$$v_r(r_0) = -\frac{\zeta\Delta\mu_1^2\beta_1\beta_2}{16\eta^2\chi}a + \frac{\zeta\Delta\mu r_0}{2\eta} \ . \tag{37}$$

A direct comparison of the ring velocity with the experiments using $a = 2\mu$m, $\beta_1 = 2$ and $\beta_2 = \eta$, leads to the values $\zeta\Delta\mu_1/\eta = 0.5s^{-1}$ and $\zeta\Delta\mu_1/\chi = .3$ which are used in Fig.14.

We now turn to the study of the formation of the contractile ring during cytokinesis [45]. Prior to the formation of the contractile ring, the cell is a sphere of radius R. The direction of the poles is perpendicular to the plane of division of the chromosomes during mitosis. We use here spherical coordinates with the pole direction as a reference axis. The angle θ vanishes at one of the poles and is equal to π at the other pole. The equator of the cell is the circle corresponding to $\theta = \pi/2$. At the beginning of cytokinesis, an excess of myosin motors is recruited along the equator in the region where the contractile ring will form. It has been shown experimentally that the recruitment of myosins is not connected to actin but it is rather related to an increase in the density of microtubule end points along the equator [40]. Myosin motors are carried on microtubules towars the equator by other molecular motors. The increase of the myosin density induces an increase of the active stress $\delta\zeta\Delta\mu(\theta)$. We describe this increase by the mathematical form $\delta\zeta(\theta) = \zeta_m \exp\left(-\frac{R^2\cos^2\theta}{a^2}\right)$. The size of the region around the equator where the myosins are recruited is a. Away from the equator, the active stress $\zeta\Delta\mu$ is constant and it is equivalent to a cortical tension $T = e\zeta\Delta\mu/2$ where e is the thickness of the actin cortex. This tension maintains the cell spherical. The increased activity along the equator of the cell tends to pinch the cell. It is the competition between these two effects which monitors the formation of the cleavage furrow. The dynamic equations for the formation of the con-

tractile ring and the cleavage furrow are obtained along the lines followed to obtain the dynamic equations for wound healing in the xenopus embryo. They must however be written on the surface of the spherical cell in spherical coordinates for the velocity field along the cell surface and the nematic order parameter. When the actin ring forms, the spherical cell is deformed and contracted at the equator. There is therefore a third dynamical equation associated to force balance in the radial direction which determines the cell deformation. The actual solution of these equations requires an expansion of all quantities in Legendre polynomials. These equations have been solved numerically and the results are displayed on figure Fig.15. As in the case of wound healing, there is a cortical flow

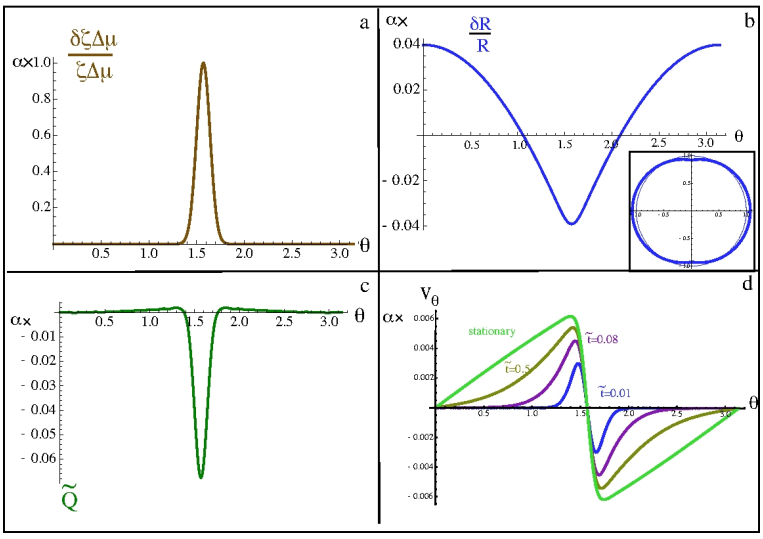

Figure 15: Formation of a contractile ring during cytokinesis. a-Active stress profile. b-Deformation of the cell around a spherical shape. c-Nematic order parameter. d-Velocity profile. All the curves are plotted as a function of the angle θ

from the pole to the equator. If the increase in activity is switched on at time $t = 0$, the velocity is first located in the vicinity of the equator and then spreads towards the pole. At long times, a steady state is reached. The orientation of the actin filaments is again coupled to the flow. Away from the equator, the nematic order parameter is positive and the actin filaments are oriented from the pole to the equator. In the vicinity of the equator, the velocity gradient changes sign and the orientation of the actin filament changes: the nematic order parameter $\tilde{Q}$ is negative and the filaments are oriented in the ϕ direction along the equator forming thus a contractile ring. The figure also shows the cell deformation. The deformation reaches a steady state resulting from a balance between the average activity which favors a spherical shape and the increase in activity close to the equator which tends to develop the cleavage furrow.

This steady state is not observed in cell division where the cleavage furrow develops and leads to the separation of the two cells. The development of the cleavage furrow is due to non-linear effects that we have not included in the theory and which drive an instability of the steady

state. One of the possible non-linearities that could be introduced is a coupling between the activity along the equator and the orientation of the filaments. It is known experimentally that the recruitment of myosin motors is larger on parallel filaments. The activity increases then with the alignment of the filaments and this clearly makes the weakly perturbed steady state that we calculated unstable. A full non-linear theory for the formation of the contractile ring is however very complex and has not been performed.

The appearance of a cortical flow and the orientation of the actin filaments during cytokinesis has been recently studied in details by the group of Y. Wang [41]. The application of the active gel theory to the cortical actin layer that we have done here clearly shows that once there is a region of enhanced activity along the equator, the pure mechanical effects taken into account by the theory are sufficient to explain the existence of a cortical flow, the orientation of the actin filaments and the formation of a cleavage furrow.

7 Conclusion

The linear theory which we have constructed has limitations. First we have not discussed fluctuations. Fluctuations have a thermal and a non-thermal component. The thermal component can be written in a systematic, well controlled procedure from the current theory Ref.[25]. There are no added parameters. The non-thermal part can either be inferred by educated guesses or measured Refs.[47], [25]. The non-thermal fluctuations are again not universal and depend on molecular details. Related theories, written for bacterial colonies, predict giant density fluctuations observed in simulations Refs.[3, 13]. The importance of active gel fluctuations in cell behavior remains to be assessed. They could for example have a strong influence on endosome diffusion.

Second the linear hydrodynamic theory that we have presented is a "gradient expansion" valid at long length scale. It is probably relevant to the actin-myosin system involved in the biological phenomena discussed here, but it does not apply to the microtubule system since individual microtubules span basically half of the cell. This is not a problem since microtubules are thought to play very little mechanical role. They are important signaling players for which we have no generic description so far.

The last limitation, is that we have described an active gel close to equilibrium. We have already pointed out that by doing so we miss a term in the dynamical equation for the polarization which can be added easily [22]. There are other consequences: far from equilibrium the tension induced by motors renormalizes the value of the short time elastic modulus together with the contractility in a spectacular way [20, 48], $E \sim (f_s)^{\frac{3}{2}}$, $\zeta\Delta\mu \sim f_s$, where f_s is the motor stall force [48]. As a result, the ratio $\frac{\zeta\Delta\mu}{E}$ decreases like the inverse square root of the motors stall force even though both E and $\zeta\Delta\mu$ increase significantly! Thus increasing motor activity, results in a decrease of the relative contractility.

Furthermore, general barrier crossing theories tell us that the Maxwell time should decrease exponentially with the same stall force. These features help reconcile contradictory observations: some reports claim that calcium fluidifies the gel, others that it rigidifies it and increases activity. Indeed it does all of that depending on the observation time scale. At "short" time scale it rigidifies the structure, but it shortens exponentially the Maxwell time, which results in a decrease in the long time viscosity $\eta = \tau E$! Such a remark is important if one wants to understand how increasing motor activity helps us move in a dynamical diagram such as the one of Fig.10. More generally, which non-linearity should be kept in a non-linear theory is model dependent and needs close comparison with experiments.

We have shown in this review that the "active gel" theory has two virtues. First it can help extract the relevant physics involved in important biological processes such as cell motility, wound healing, cytokinesis and help getting at quantitative biology. It is interesting to remark that the orders of magnitude that we obtain for the contractility from cell motility experiments are useful to understand cell oscillations, wound healing and cytokinesis. Since the equations were obtained essentially from conservation laws and symmetry arguments they are robust and do not depend on molecular details. What depends on the protein details is the value of the parameters such as viscosity, friction coefficient and contractility. One of the main findings is that thin active gel layers such as the cortical layer, are unstable without proper feedback. It was known since the work of Hodgkin and Huxley that neural cells were electrically excitable media. We now know that most eukaryotic cells are almost mechanically excitable systems, prone to strong shape responses since they are sitting "close" to mechanical instabilities. This is probably the main reason for the observed cell plasticity. Getting to quantitative biology will require measuring the parameters that we have introduced in this macroscopic theory. Their number may look large at first sight, but there are only a few additional terms as compared to liquid crystals for which all coefficients have been measured and for which the theory has been very successful. One could also get a profound insight by studying artificial systems for which it would be easier to vary parameters. For instance it would be very useful to replace ATP by photons.

However, if the tool is useful it has it is not sufficient as it stands. We have already seen in the example of the oscillations that signaling comes into the game and is important. The second messenger calcium stabilizes the cortical layer and the feedback efficiency compared to the Maxwell time is the key feature controlling the oscillations. This feedback is not universal and depends on many details, so that even though one starts with a rather universal description the outcome depends on biological details. This is in a sense reassuring since we knew from the start that it had to, but it tells us that these details control the dynamical state of the cell, in a prescribed generic diagram. It also tells us that only a close collaboration between experiment and theory will allow to construct a quantitative description of cell behavior.

References

[1] M. Kirshner, J. Gerhart, *The Plausibility of Life: Resolving Darwin's dilemma*, Yale Uniersity Press, 2007.

[2] *et al.*. B. Alberts, *Molecular Biology of the Cell*, Garland, 2002.

[3] R. Simha, S. Ramaswamy, *Hydrodynamic fluctuations and instabilities in ordered suspensions of self-propelled particles*, Phys. Rev. Lett. **89** (2002), 058101.

[4] J. Toner, Y. Tu, *Long range order in a two-dimensional dynamical xy model: how birds fly together?*, Phys. Rev. Lett. **75** (1995), 4326–4329.

[5] I. Tuval, L. Cisneros, C. Dombrowski, C. W. Wolgemuth, J. O. Kessler, R. E. Goldstein, *Bacterial swimming and oxygen transport near contact lines*, Proc Natl Acad Sci U S A **102** (7) (2005), 2277–2282.
URL `http://dx.doi.org/10.1073/pnas.0406724102`

[6] J. Prost, Conference solvay, in: Chemistry of molecular motors, 2007.

[7] F. J. Nedelec, T. Surrey, A. C. Maggs, S. Leibler, *Self-organization of microtubules and motors*, Nature **389** (6648) (1997), 305–308.
URL `http://dx.doi.org/10.1038/38532`

[8] A. Mogilner, G. Oster, *The physics of lamellipodial protrusion*, Eur. Biophys. J. **25** (1996), 47–53.

[9] T. B. Liverpool, M. C. Marchetti, *Instabilities of isotropic solutions of active polar filaments*, Phys. Rev. Lett. **90** (2003), 138102.

[10] A. Ahmadi, T. Liverpool, M. Marchetti, *Nematic and polar order in active filament solutions*, Phys. Rev. E Stat. Nonlin. Soft Matter Phys. **72** (2005), 060901.

[11] I. Aranson, L. S. Tsimring, *Pattern formation of microtubules and motors: Inelastic interaction of polar rods*, Phys. Rev. E **71** (2005), 050901 (R).

[12] K. Kruse, F. Julicher, *Actively contracting bundles of polar filaments*, Phys. Rev. Lett. **85** (8) (2000), 1778–1781.

[13] H. Chate, F. Ginelli, R. Montagne, *Simple model for active nematics: quasi-long-range order and giant fluctuations*, Phys. Rev. Lett. **96** (18), (2006) 180602.

[14] K. Kruse, J. F. Joanny, F. Julicher, J. Prost, K. Sekimoto, *Asters, vortices, and rotating spirals in active gels of polar filaments*, Phys. Rev. Lett. **92** (7) (2004), 078101.

[15] K. Kruse, J. Joanny, F. Julicher, J. Prost, K. Sekimoto, *Generic theory of active polar gels: a paradigm for cytoskeletal dynamics*, Eur. Phys. J. E **16** (2005), 5–16.

[16] F. Julicher, K. Kruse, J. Prost, J. F. Joanny, *Active behavior of the cytoskeleton*, Physics Reports **449** (2007), 3–28.

[17] T.Svitkina, G.G.Borisi, *Correlative light and electron microscopy of the cytoskeleton of cultured cells*, Methods Enzymol. **298** (1998), 570–592.

[18] P. DeGennes, J. J. Prost, *The Physics of Liquid crystals*, Oxford University Press, 1993.

[19] K. Takiguchi, *Heavy meromyosin induces sliding movements between antiparallel actin filaments*, J. Biochem. **109** (4) (1991), 520–527.

[20] P. M. Bendix, G. H. Koenderink, D. Cuvelier, Z. Dogic, B. N. Koeleman, W. M. Brieher, C. M. Field, L. Mahadevan, D. A. Weitz, *A quantitative analysis of contractility in active cytoskeletal protein networks*, Biophys. J. **94** (8) (2008), 3126–3136.
URL `http://dx.doi.org/10.1529/biophysj.107.117960`

[21] Y. Hatwalne, S. Ramaswamy, M. Rao, R. Simha, *Rheology of active-particle suspensions*, Phys. Rev. Lett. **92** (2004), 118101.

[22] L. Giomi, M. C. Marchetti, T. Liverpool, *Complex spontaneous flows and concentration banding in active polar films*, Phys. Rev. Lett. (2008).

[23] R. Voituriez, J. Joanny, J. J. Prost, *Spontaneous flow transtions in active polar gels*, Europhys. Lett. **70** (2005), 404–410.

[24] R. Voituriez, J. F. Joanny, J. Prost, *Generic phase diagram of active polar films*, Phys. Rev. Lett. **96** (2) (2006), 028102.

[25] A. . Basu, J. Joanny, F. Julicher, J. J. Prost, *Thermal and non-thermal fluctuations in active polar gels*, submitted to European Physical Journal E (2008).

[26] G. Toulouse, M. Kleman, *Principles of a classification of defects in ordered media*, J. Phys. Lett. **37** (1976), 149–151.

[27] J. Prost, C. Barbetta, J.-F. Joanny, *Dynamical control of the shape and size of stereocilia and microvilli*, Biophys. J. **93** (4) (2007), 1124–1133.
URL `http://dx.doi.org/10.1529/biophysj.106.098038`

[28] W. Helfrich, *Elastic properties of lipid bilayers: thoery and possible experiments*, Zeirschrift fur Naturforschung C **28** (11–1) (1973), 693–703.

[29] A. Mogilner, G. Oster, *The polymerization ratchet model explains the force-velocity relation for growing microtubules*, Eur. Biophys. J. **28** (1999), 235–242.

[30] A. E. Carlsson, *Growth velocities of branched actin networks*, Biophys. J. **84** (5) (2003), 2907–2918.

[31] P. Vallotton, G. Danuser, S. Bohnet, J.-J. Meister, A. B. Verkhovsky, *Tracking retrograde flow in keratocytes: news from the front*, Mol. Biol. Cell. **16** (3) (2005), 1223–1231.
URL http://dx.doi.org/10.1091/mbc.E04-07-0615

[32] F. Gerbal, P. Chaikin, Y. Rabin, J. Prost, *An elastic analysis of listeria monocytogenes propulsion*, Biophys. J. **79** (5) (2000), 2259–2275.

[33] K. Sekimoto, K. Tawada, *Fluctuations in sliding motion generated by independent and random actions of protein motors*, Biophys. Chem. **89** (1) (2001), 95–99.

[34] A. C. Callan-Jones, J.-F. Joanny, J. Prost, *Viscous-fingering-like instability of cell fragments*, Phys. Rev. Lett. **100** (25) (2008), 258106.

[35] K. Kruse, J. F. Joanny, F. Julicher, J. Prost, *Contractility and retrograde flow in lamellipodium motion*, Phys. Biol. **3** (2) (2006), 130–137.
URL http://dx.doi.org/10.1088/1478-3975/3/2/005

[36] Y. Marcy, J. Prost, M.-F. Carlier, C. Sykes, *Forces generated during actin-based propulsion: a direct measurement by micromanipulation*, Proc. Natl. Acad. Sci. U S A **101** (16) (2004), 5992–5997.
URL http://dx.doi.org/10.1073/pnas.0307704101

[37] E. Paluch, M. Piel, J. Prost, M. Bornens, C. Sykes, *Cortical actomyosin breakage triggers shape oscillations in cells and cell fragments*, Biophys. J. **89** (1) (2005), 724–733.
URL http://dx.doi.org/10.1529/biophysj.105.060590

[38] G. Salbreux, J. F. Joanny, J. Prost, P. Pullarkat, *Shape oscillations of non-adhering fibroblast cells*, Phys. Biol. **4** (4) (2007), 268–284.
URL http://dx.doi.org/10.1088/1478-3975/4/4/004

[39] I. Pletjushkina, Z. Rajfur, P. Pomorski, T. Oliver, J. Vasiliev, K. Jacobson, *Induction of cortical oscillations in spreading cells by depolymerization of microtubules*, Cell Motility and the Cytoskeleton **48** (2001), 235–244.

[40] J. H. Zang, J. A. Spudich, *Myosin ii localization during cytokinesis occurs by a mechanism that does not require its motor domain*, Proc. Natl. Acad. Sci. U S A **95** (23) (1998), 13652–13657.

[41] M. Zhou, Y.-L. Wang, *Distinct pathways for the early recruitment of myosin ii and actin to the cytokinetic furrow*, Mol. Biol. Cell. **19** (1) (2008), 318–326.
URL http://dx.doi.org/10.1091/mbc.E07-08-0783

[42] D. J. Fishkind, Y. L. Wang, *Orientation and three-dimensional organization of actin filaments in dividing cultured cells*, J. Cell. Biol. **123** (4) (1993), 837–848.

[43] C. Mandato, W. Bement, *Contraction and polymerization cooperate to assemble and close actomyosin rings around xenopus oocyte wounds*, J. Cell. Biol. **154** (2001), 785–797.

[44] C. A. Mandato, W. M. Bement, *Actomyosin transports microtubules and microtubules control actomyosin recruitment during xenopus oocyte wound healing*, Curr. Biol. **13** (13) (2003), 1096–1105.

[45] G. Salbreux, J. Prost, J.F. Joanny, *Hydrodynamics of cellular cortical flows and formation of contractile rings*, Phys. Rev. Lett. (2009).

[46] G. Debregeas, P. Martin, F. Brochard-Wyart, *Viscous bursting of suspended films*, Phys. Rev. Lett. **75** (21) (1995), 3886–38.

[47] D. Mizuno, C. Tardin, C. Schmidt, F. MacKintosh, *Nonequilibrium Mechanics of Active Cytoskeletal Networks*, Science **315** (2007), 370–373.

[48] T. Liverpool, C. Marchetti, J.-F. Joanny, J. Prost, *Mechanical Response of Active Gels*, Europhysics Letters in press (2009).